Monotone meshfree methods for linear elliptic equations in non-divergence form via nonlocal relaxation

Qihao Ye* Xiaochuan Tian

University of California, San Diego (UCSD)

October, 2023

The 8th Annual Meeting of SIAM Central States Section

Manuscript: http://doi.org/10.1007/s10915-023-02294-3

Outline

Outline

Main Goal

Solve the second-order linear elliptic equation in non-divergence form

$$\begin{cases} -Lu(\boldsymbol{x}) := -\sum_{i,j=1}^{d} a^{ij}(\boldsymbol{x})\partial_{ij}u(\boldsymbol{x}) = f(\boldsymbol{x}) & \boldsymbol{x} \in \Omega \\ u(\boldsymbol{x}) = g(\boldsymbol{x}) & \boldsymbol{x} \in \partial\Omega \end{cases},$$

for an open bounded domain $\Omega \subset \mathbb{R}^d$. The matrix $A(\boldsymbol{x}) = (a^{ij}(\boldsymbol{x}))_{i,j=1}^{d}$ is assumed to be symmetric and positive definite satisfying the uniform ellipticity condition

$$\lambda|\boldsymbol{\xi}|^2 \leq \boldsymbol{\xi}^T A(\boldsymbol{x})\boldsymbol{\xi} \leq \Lambda|\boldsymbol{\xi}|^2 \qquad \forall \boldsymbol{\xi} \in \mathbb{R}^d, \forall \boldsymbol{x} \in \Omega,$$

for positive constants λ, Λ with ratio $\varrho := \lambda/\Lambda \leq 1$.
Denote $M(\boldsymbol{x}) := (A(\boldsymbol{x}))^{1/2}$.

Applications

Non-divergence form elliptic equations

- Arise in probablity and stochastic processes[1]
- Are linearizations of Hamilton-Jacobi-Bellman (HJB) equations (with applications in the fields of optimal control and finance)[2]
- Are linearizations of the Monge-Ampère equation (with applications to the optimal transportation problem and geometry)[3]

[1] [Cabré, 2008, Fleming and Soner, 2006]
[2] [Fleming and Soner, 2006]
[3] [Caffarelli and Gutiérrez, 1997]

Main Challenges

1. In general, the equation cannot be recast into a divergence form
$$-\mathrm{div}(\tilde{A}(\boldsymbol{x})\nabla u) + \boldsymbol{b}(\boldsymbol{x}) \cdot \nabla u,$$
e.g. when $A(\boldsymbol{x})$ is discontinuous.
We cannot easily apply FEM to solve the equation in non-divergence form.

2. When $\varrho \ll 1$, the equation is near degenerate. Maximum principle preserving finite difference method in general requires wide stencils[4].

[4] [Kocan, 1995] gave an estimate of the stencil width for the existence of positive-type finite difference method, and it grows ϱ^{-1} in 2d (similarly in a recent work [Mirebeau, 2016]) and $\varrho^{-5/2}$ in 3d.

Our Work

Main Idea:

Nonlocal Relaxation
+
Robust Discretization

$$
\begin{tikzcd}
 & L & \\
\mathcal{L}_\delta \arrow[u, "\delta \to 0"] \arrow[rr, "\text{discretize}"'] & & \mathcal{L}_\delta^h \arrow[ul, "\delta = \Theta(h)"']
\end{tikzcd}
$$

Main Results:

1. Monotone meshfree method: has guaranteed convergence.
2. Significant improvement in theoretical analysis of the existence of positive stencils ($\varrho^{-1/2}$ stencil width growth for both 2d and 3d).
3. Practical: sparse linear system, successfully implemented in 2d and 3d for a variety of geometries and coefficient matrices $A(\boldsymbol{x})$, applicable to the near-degenerate regime $\varrho \ll 1$, new experiments on degenerate elliptic equations.

Nonlocal Relaxation to Elliptic Equations

When $A(\boldsymbol{x}) = I_{d\times d}$, we get the Laplace operator:

$$\Delta u(\boldsymbol{x}) = \sum_{i=1}^{d} \partial_{ii} u(\boldsymbol{x}).$$

The nonlocal Laplace operator[5] is given by

$$\tilde{\mathcal{L}}_\delta u(\boldsymbol{x}) = \int_{B_\delta(\mathbf{0})} \frac{1}{\delta^{d+2}} \gamma\left(\frac{|\boldsymbol{y}|}{\delta}\right) (u(\boldsymbol{x}+\boldsymbol{y}) - u(\boldsymbol{x}))\, d\boldsymbol{y},$$

where γ is a nonnegative kernel with

$$\int_{B_1(\mathbf{0})} |\boldsymbol{y}|^2 \gamma(|\boldsymbol{y}|)\, d\boldsymbol{y} = 2d.$$

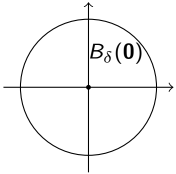

[5] [Du et al., 2012, Silling, 2000]

Nonlocal Relaxation to Elliptic Equations

$$\tilde{\mathcal{L}}_\delta u(\boldsymbol{x}) = \int_{B_\delta(\boldsymbol{0})} \frac{1}{\delta^{d+2}} \gamma\left(\frac{|\boldsymbol{y}|}{\delta}\right) \left(u(\boldsymbol{x}+\boldsymbol{y}) - u(\boldsymbol{x})\right) d\boldsymbol{y},$$

It can be shown that

$$\tilde{\mathcal{L}}_\delta u(\boldsymbol{x}) \to \Delta u(\boldsymbol{x}) \qquad \text{as} \quad \delta \to 0.$$

Nonlocal Relaxation to Elliptic Equations

For general $A(\boldsymbol{x})$, the nonlocal elliptic operator[6] can be defined as

$$\begin{aligned}\mathcal{L}_\delta u(\boldsymbol{x}) &= \int_{B_\delta(\mathbf{0})} \frac{1}{\delta^{d+2}}\gamma\left(\frac{|\boldsymbol{z}|}{\delta}\right)(u(\boldsymbol{x}+M(\boldsymbol{x})\boldsymbol{z})-u(\boldsymbol{x}))\,d\boldsymbol{z}\\ &= \int_{\mathcal{E}_\delta^{\boldsymbol{x}}(\mathbf{0})} \frac{1}{\delta^{d+2}}\gamma\left(\frac{|M(\boldsymbol{x})^{-1}\boldsymbol{y}|}{\delta}\right)\det(M(\boldsymbol{x}))^{-1}(u(\boldsymbol{x}+\boldsymbol{y})-u(\boldsymbol{x}))\,d\boldsymbol{y}\\ &:= \int_{\mathcal{E}_\delta^{\boldsymbol{x}}(\mathbf{0})} \rho_\delta(\boldsymbol{x},\boldsymbol{y})(u(\boldsymbol{x}+\boldsymbol{y})-u(\boldsymbol{x}))\,d\boldsymbol{y}.\end{aligned}$$

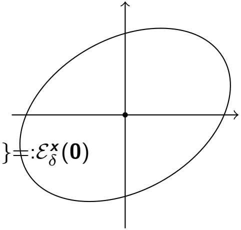

[6] [Nochetto and Zhang, 2018]

Nonlocal Relaxation to Elliptic Equations

$$
\begin{aligned}
\mathcal{L}_\delta u(\boldsymbol{x}) &= \int_{B_\delta(\mathbf{0})} \frac{1}{\delta^{d+2}}\gamma\left(\frac{|\boldsymbol{z}|}{\delta}\right)(u(\boldsymbol{x}+M(\boldsymbol{x})\boldsymbol{z})-u(\boldsymbol{x}))\,d\boldsymbol{z}\\
&= \int_{\mathcal{E}_\delta^{\boldsymbol{x}}(\mathbf{0})} \frac{1}{\delta^{d+2}}\gamma\left(\frac{|M(\boldsymbol{x})^{-1}\boldsymbol{y}|}{\delta}\right)\det(M(\boldsymbol{x}))^{-1}(u(\boldsymbol{x}+\boldsymbol{y})-u(\boldsymbol{x}))\,d\boldsymbol{y}\\
&:= \int_{\mathcal{E}_\delta^{\boldsymbol{x}}(\mathbf{0})} \rho_\delta(\boldsymbol{x},\boldsymbol{y})(u(\boldsymbol{x}+\boldsymbol{y})-u(\boldsymbol{x}))\,d\boldsymbol{y}.
\end{aligned}
$$

It can be shown that

$$
\mathcal{L}_\delta u(\boldsymbol{x}) \to Lu(\boldsymbol{x}) \qquad \text{as} \quad \delta \to 0.
$$

Minimal Positive Stencil

$$\begin{cases} \text{minimal} & \Longrightarrow & \text{sparsity} \\ \text{positive} & \Longrightarrow & \text{stability} \end{cases}$$

We usually use **truncation error** to analyze the consistency of a method. Then if the method also satisfies the **discrete maximum principle**, according to the Lax equivalence theorem, we will have a convergent method.

Minimal Positive Stencil

Minimal stencils are beneficial for the sparsity of the linear system matrix, resulting in a lower memory consumption and a faster solution of a linear system.

In formula

$$\mathcal{L}_\delta^h u(\boldsymbol{x}_i) = \sum_{\boldsymbol{x}_j \in \mathcal{N}(\boldsymbol{x}_i)} \beta_{j,i} \Big(u(\boldsymbol{x}_j) - u(\boldsymbol{x}_i) \Big)$$

where $\mathcal{N}(\boldsymbol{x}_i)$ is some neighborhood of $\boldsymbol{x}_i$,
we need a small $\#\{j : \beta_{j,i} \neq 0\}$.

Minimal Positive Stencil

We aim to obtain a **positive** stencil, because a positive stencil automatically satisfies the discrete maximum principle.

In formula

$$\mathcal{L}_\delta^h u(\boldsymbol{x}_i) = \sum_{\boldsymbol{x}_j \in \mathcal{N}(\boldsymbol{x}_i)} \beta_{j,i} \Big(u(\boldsymbol{x}_j) - u(\boldsymbol{x}_i) \Big)$$

we need $\beta_{j,i} \geq 0$ for all j.

Outline

Notations

Let Ω_δ be the extended domain.
Point cloud $X = \{\boldsymbol{x}_1, \ldots, \boldsymbol{x}_M\} \subset \Omega_\delta$ be given. Meshfree just means that no information about connection of points is provided.

Point cloud contains two types of points:

1. Interior points $\{\boldsymbol{x}_1, \ldots, \boldsymbol{x}_N\}$ (in Ω),
2. Boundary points $\{\boldsymbol{x}_{N+1}, \ldots, \boldsymbol{x}_M\}$ (in $\Omega_\delta \setminus \Omega$).

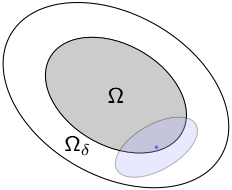

For each interior point, two steps are needed:

1. Define which points are its neighbors (vary for $A(\boldsymbol{x})$),
2. Select a stencil (using a minimization problem).

Boundary Treatment

We consider each boundary point $\boldsymbol{x}_j$ around $\boldsymbol{x}_i$ as the closest projection $\boldsymbol{y}_{j,i}$ from $\boldsymbol{x}_j$ to $\boldsymbol{x}_i$ at the boundary.

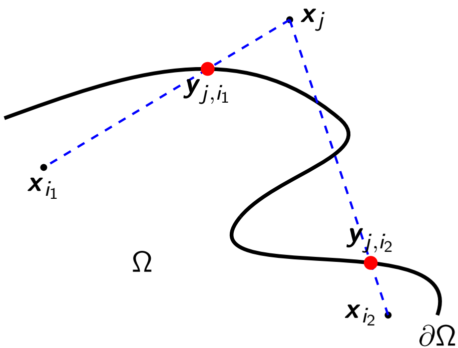

Then apply the boundary condition to these mapped boundary points to proceed.

Moving Least Squares

Moving least squares method[7] finds a unique stencil via a quadratic minimization problem, take the approximation of Laplace operator as an example:

$$\{\beta_{j,i}\} = \arg\min_{\{\beta_{j,i}\}\in S_{\delta,h,p}(\boldsymbol{x}_i)} \sum_j \frac{\beta_{j,i}^2}{W_\delta(|\boldsymbol{x}_j - \boldsymbol{x}_i|)},$$

where

$$S_{\delta,h,p}(\boldsymbol{x}_i) := \left\{ \{\beta_{j,i}\} : \tilde{\mathcal{L}}_\delta^h u(\boldsymbol{x}_i) = \tilde{\mathcal{L}}_\delta u(\boldsymbol{x}_i)\ \forall u \in \mathcal{P}_p(\mathbb{R}^d) \right\},$$

$$W_\delta(|\boldsymbol{x}_j - \boldsymbol{x}_i|) = \frac{1}{\delta^{d+2}} \gamma \left(\frac{|\boldsymbol{x}_j - \boldsymbol{x}_i|}{\delta} \right),$$

$$\tilde{\mathcal{L}}_\delta^h u(\boldsymbol{x}_i) = \sum_{\boldsymbol{x}_j \in B_\delta(\boldsymbol{x}_i)} \beta_{j,i}(u(\boldsymbol{x}_j) - u(\boldsymbol{x}_i)); \quad \tilde{\mathcal{L}}_\delta u(\boldsymbol{x}) \to \Delta u(\boldsymbol{x}) \quad \text{as} \quad \delta \to 0.$$

[7] [Liu et al., 1996, Mirzaei et al., 2012, Trask et al., 2019]

Moving Least Squares

$$\{\beta_{j,i}\} = \underset{\{\beta_{j,i}\}\in S_{\delta,h,p}(\boldsymbol{x}_i)}{\arg\min} \sum_j \frac{\beta_{j,i}^2}{W_\delta(|\boldsymbol{x}_j - \boldsymbol{x}_i|)},$$

1. In general, least squares approaches do not select minimal stencils.
2. When ϱ is small, the number of points in the neighborhood grows very large, therefore quadratic minimization results in a much denser system.
3. In general, least squares approaches do not select positive stencils.

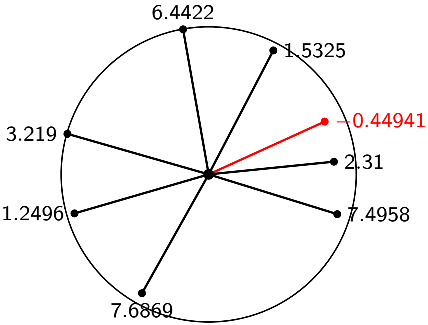

ℓ_1 Type Minimization Problem

We use the following minimization problem[8] to select a unique stencil for interior point $\boldsymbol{x}_i$ and p the order of the polynomial space:

$$\{\beta_{j,i}\} = \operatorname*{arg\,min}_{\{\beta_{j,i}\} \in S_{\delta,h,p}(\boldsymbol{x}_i)} \sum_j \frac{\beta_{j,i}}{\rho_\delta(\boldsymbol{x}_i, \boldsymbol{x}_j - \boldsymbol{x}_i)},$$

where

$$S_{\delta,h,p}(\boldsymbol{x}_i) := \left\{ \{\beta_{j,i}\} : \beta_{j,i} \geq 0 \text{ and } \mathcal{L}_\delta^h u(\boldsymbol{x}_i) = \mathcal{L}_\delta u(\boldsymbol{x}_i) \ \forall u \in \mathcal{P}_p(\mathbb{R}^d) \right\},$$

$$\mathcal{L}_\delta^h u(\boldsymbol{x}_i) = \sum_{\boldsymbol{x}_j \in \mathcal{E}_\delta^{\boldsymbol{x}_i}(\boldsymbol{x}_i)} \beta_{j,i}(u(\boldsymbol{x}_j) - u(\boldsymbol{x}_i)).$$

[8] [Seibold, 2008, Davydov and Schaback, 2018]

ℓ_1 Type Minimization Problem

$$\{\beta_{j,i}\} = \underset{\{\beta_{j,i}\}\in S_{\delta,h,p}(\boldsymbol{x}_i)}{\arg\min} \sum_j \frac{\beta_{j,i}}{\rho_\delta(\boldsymbol{x}_i, \boldsymbol{x}_j - \boldsymbol{x}_i)},$$

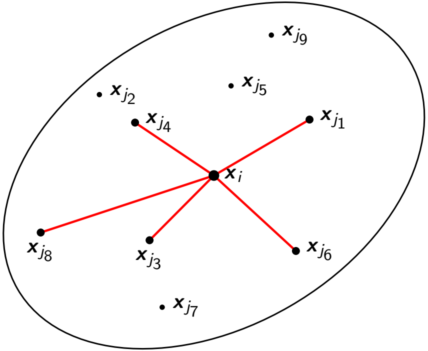

ℓ_1 Type Minimization Problem

To include the projection for all boundary points, define

$$\boldsymbol{y}_{j,i} = \begin{cases} \boldsymbol{x}_j & , \boldsymbol{x}_j \in \overline{\Omega} \\ \text{projection from } \boldsymbol{x}_j \text{ to } \boldsymbol{x}_i \text{ at } \partial\Omega & , \boldsymbol{x}_j \in \Omega_\delta \setminus \overline{\Omega} \end{cases}$$

and

$$\overline{S}_{\delta,h,p}(\boldsymbol{x}_i) := \left\{ \{\beta_{j,i}\} : \beta_{j,i} \geq 0 \text{ and } \mathcal{L}^h_{\delta,\Omega} u(\boldsymbol{x}_i) = \mathcal{L}_\delta u(\boldsymbol{x}_i)\ \forall u \in \mathcal{P}_p(\mathbb{R}^d) \right\},$$

$$\mathcal{L}^h_{\delta,\Omega} u(\boldsymbol{x}_i) = \sum_{\boldsymbol{x}_j \in \mathcal{E}^{\boldsymbol{x}_i}_\delta(\boldsymbol{x}_i)} \beta_{j,i}(u(\boldsymbol{y}_{j,i}) - u(\boldsymbol{x}_i)).$$

ℓ_1 Type Minimization Problem

Then the minimization problem becomes $\{\beta_{j,i}\} = \underset{\{\beta_{j,i}\}\in\overline{S}_{\delta,h,p}(\boldsymbol{x}_i)}{\arg\min} \sum_j \frac{\beta_{j,i}}{\rho_\delta(\boldsymbol{x}_i, \boldsymbol{y}_{j,i} - \boldsymbol{x}_i)}$,

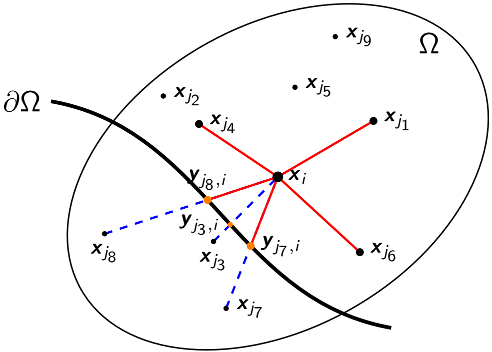

Existence of Solution Condition

Theorem 1 (Ye-Tian, 2023)

In $d = 2$ or $d = 3$, there exists a positive constant c (which only depends on d)[9] such that if

$$\delta \geq c h \varrho^{-1/2},$$

then $S_{\delta,h,2}(\boldsymbol{x}_i)$ and $\overline{S}_{\delta,h,2}(\boldsymbol{x}_i)$ are not empty.

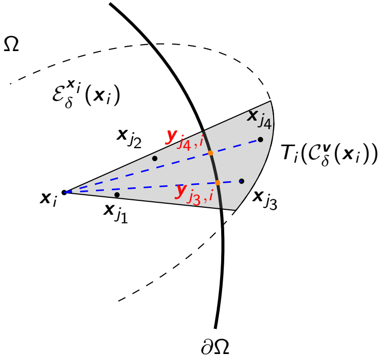

[9] In our manuscript, $c = 3.614$ in 2d and $c = 4.450$ in 3d.

Significance/Implication of the Previous Theorem

1. For a fixed ϱ, $\delta = \Theta(h)$, which is a robust discretization.
2. When $\varrho \to 0$, the stencil width is $\varrho^{-1/2}$. The size of the elliptic region is near-optimal.[10]

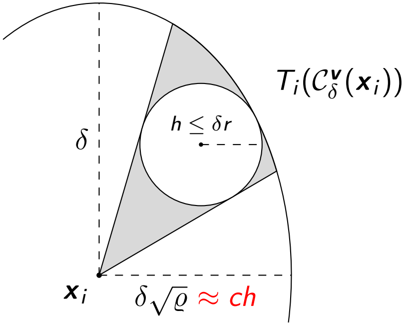

[10] This theorem significantly improves the results in [Kocan, 1995] and [Mirebeau, 2016].

Convergence Estimate

Theorem 2 (Ye-Tian, 2023)

In $d = 2$ or $d = 3$, assume $\overline{S}_{\delta,h,p}(\boldsymbol{x}_i)$ is not empty, let u be the real solution and u_δ^h be the solution solved by the discrete operator and $C > 0$ is a generic constant.

1. *If $p \geq 2$ and $u \in C^{2,\alpha}(\overline{\Omega})$ for $\alpha \in (0, 1]$, then*
$$\max_{\boldsymbol{x}_i \in \Omega} \left| u(\boldsymbol{x}_i) - u_\delta^h(\boldsymbol{x}_i) \right| \leq C |u|_{C^{2,\alpha}(\overline{\Omega})} \left(\sqrt{\varrho}\right)^{-\alpha} h^\alpha.$$
2. *If $p \geq 3$ and $u \in C^{3,\alpha}(\overline{\Omega})$ for $\alpha \in (0, 1]$, then*
$$\max_{\boldsymbol{x}_i \in \Omega} \left| u(\boldsymbol{x}_i) - u_\delta^h(\boldsymbol{x}_i) \right| \leq C |u|_{C^{3,\alpha}(\overline{\Omega})} \left(\sqrt{\varrho}\right)^{-(1+\alpha)} h^{1+\alpha}.$$

Outline

Domains

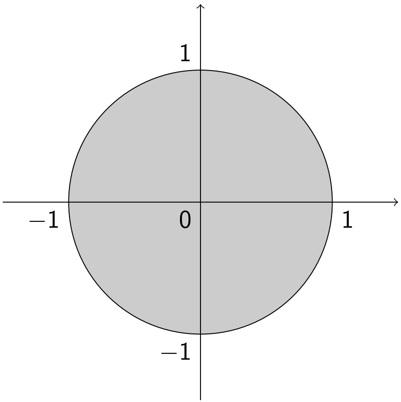

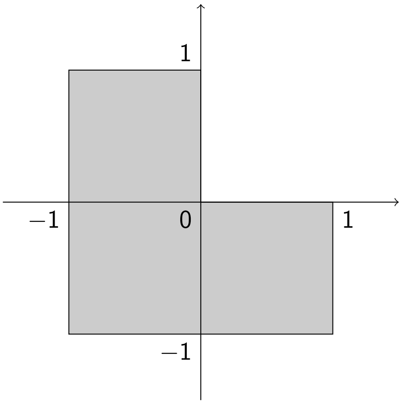

Continuous Coefficient Matrices

#	$A(\boldsymbol{x})$	λ/Λ for $\boldsymbol{x}\in[-1,1]^2$
0	$\begin{pmatrix} 1 & 0 \\ 0 & 1 \end{pmatrix}$	1.0000
1	$\begin{pmatrix} 1-0.5\lvert x_1\rvert & 0 \\ 0 & 0.25+0.25\lvert x_2\rvert \end{pmatrix}$	0.2500
2	$\frac{1}{2.21}\begin{pmatrix} 2-\lvert x_1\rvert & 0.5 \\ 0.5 & 0.5+0.5\lvert x_2\rvert \end{pmatrix}$	0.0864
3	$\begin{pmatrix} 1-0.5\lvert x_1\rvert & 0 \\ 0 & 0.025+0.025\lvert x_2\rvert \end{pmatrix}$	0.0250
4	$\begin{pmatrix} 1-0.5\lvert x_1\rvert & 0 \\ 0 & 0.0025+0.0025\lvert x_2\rvert \end{pmatrix}$	0.0025
5	$\frac{1}{2.001}\begin{pmatrix} 2-\lvert x_1(0.5-x_2)\rvert & 0.025 \\ 0.025 & 0.01+0.0025\lvert x_1\exp(x_2)\rvert \end{pmatrix}$	0.0014

Error Graph for Continuous Coefficient Matrices

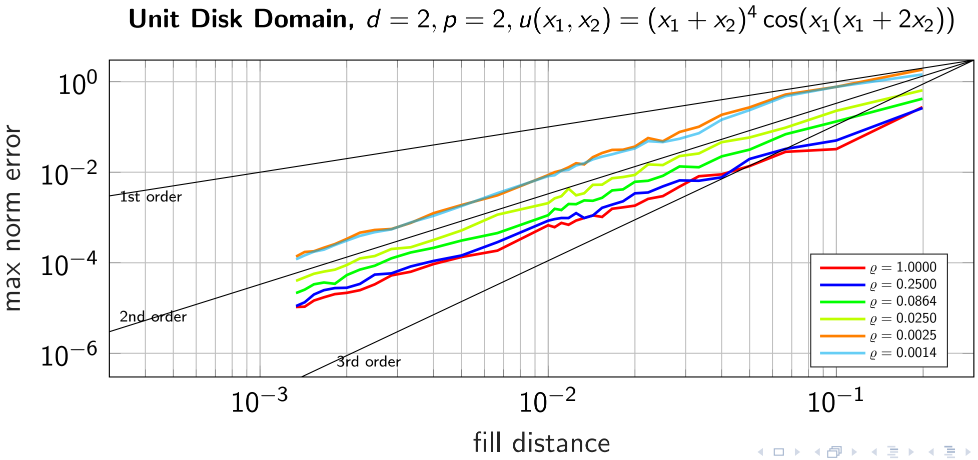

Error Graph for Continuous Coefficient Matrices

L-shaped Domain, $d = 2, p = 2, u(x_1, x_2) = (x_1 + x_2)^4 \cos(x_1(x_1 + 2x_2))$

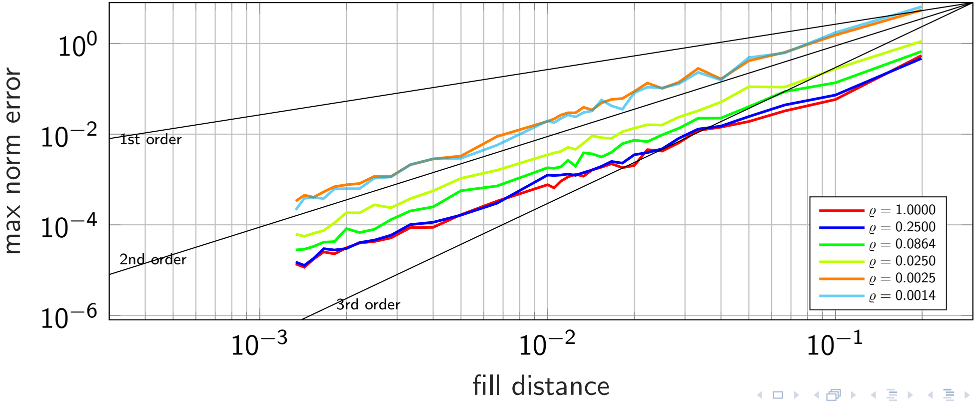

Discontinuous Coefficient Matrices

Divide the domain into blocks and define piecewise constant coefficient matrices with respect to the blocks.

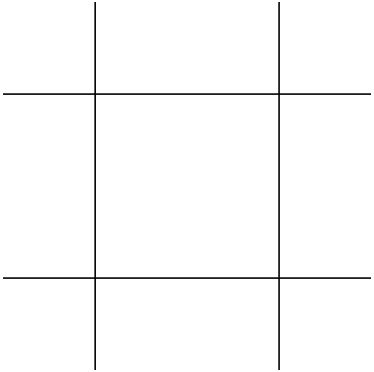

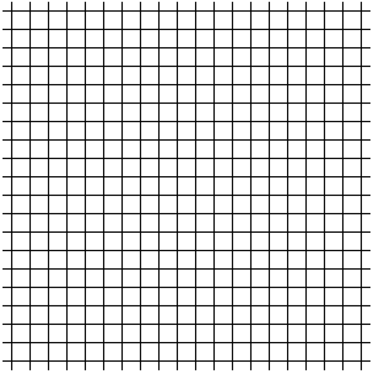

Discontinuous Coefficient Matrices

We tested for the following $A(\boldsymbol{x})$:

#	discription	λ/Λ for $\boldsymbol{x} \in [-1,1]^2$
6	dense blocks	0.2500
7	medium blocks	0.2500
8	loose blocks	0.2500

We also tested the combination of previous matrices:

$$A_9(\boldsymbol{x}) = \begin{cases} A_2(\boldsymbol{x}), & x_1 < 0 \\ A_3(\boldsymbol{x}), & \text{otherwise} \end{cases} \quad \text{with} \quad \begin{array}{l} \lambda/\Lambda = 0.0250 \\ \text{for } \boldsymbol{x} \in [-1,1]^2 \end{array}$$

Error Graph for Discontinuous Coefficient Matrices

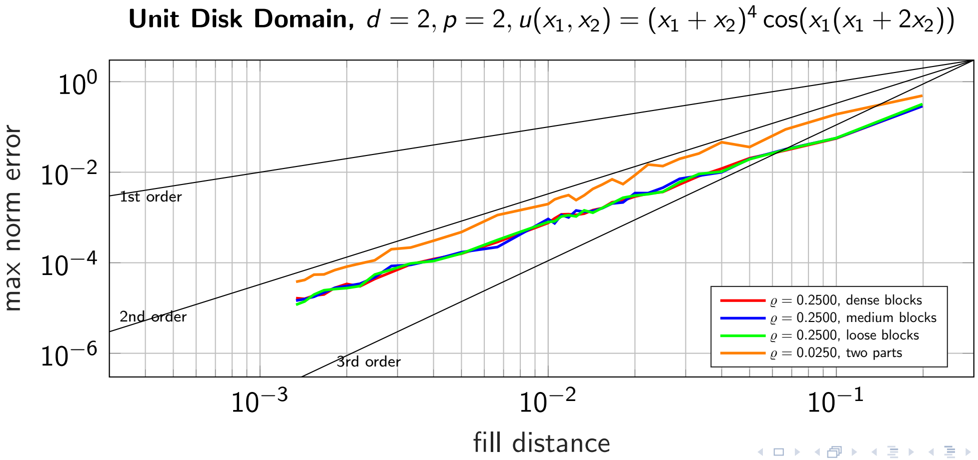

Error Graph for Discontinuous Coefficient Matrices

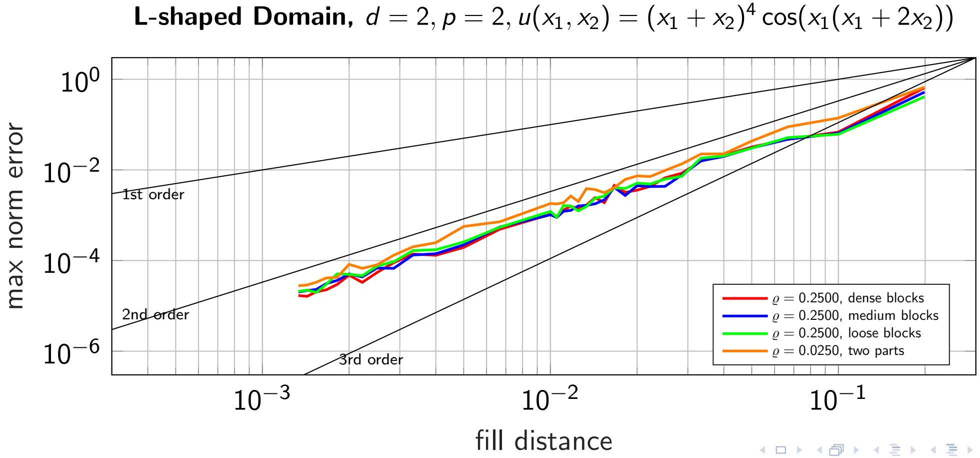

Domains

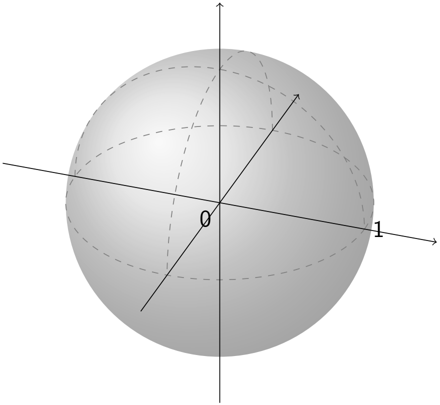

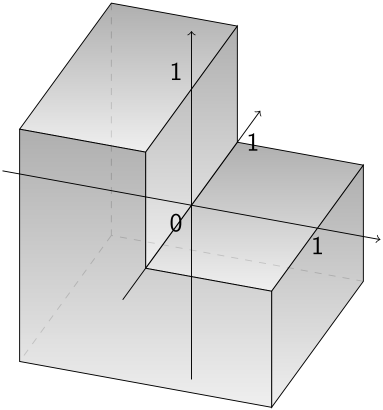

Error Graph for Continuous Coefficient Matrices

Unit Sphere Domain, $d = 3, p = 2, u(x_1, x_2, x_3) = (x_1 + x_2 + x_3)^4 \cos(x_1(x_1 + 2x_2 + 2x_3))$

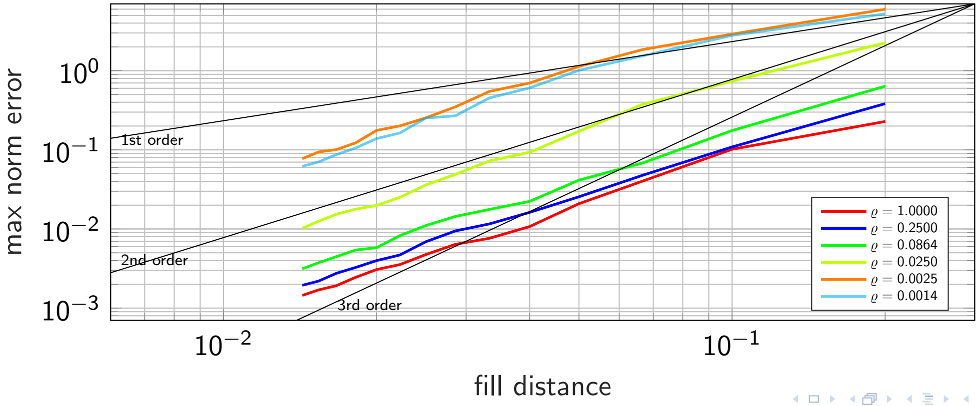

Error Graph for Continuous Coefficient Matrices

3d L-shaped Domain, $d = 3, p = 2, u(x_1, x_2, x_3) = (x_1 + x_2 + x_3)^4 \cos(x_1(x_1 + 2x_2 + 2x_3))$

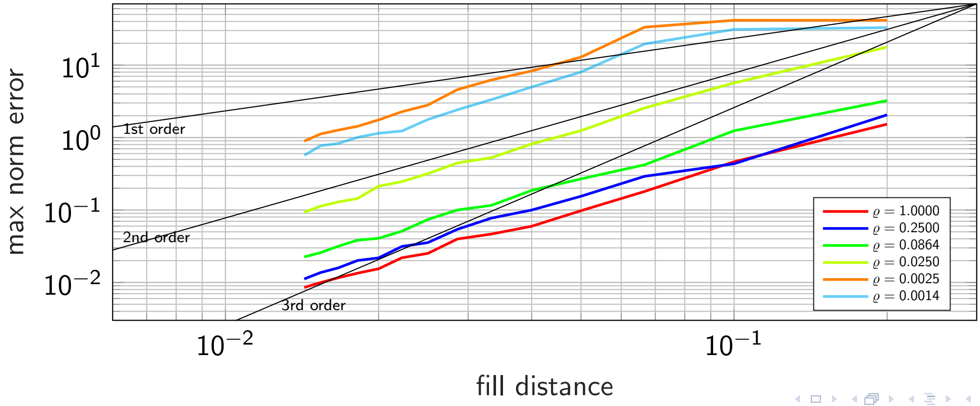

Error Graph for Discontinuous Coefficient Matrices

Unit Sphere Domain, $d = 3, p = 2, u(x_1, x_2, x_3) = (x_1 + x_2 + x_3)^4 \cos(x_1(x_1 + 2x_2 + 2x_3))$

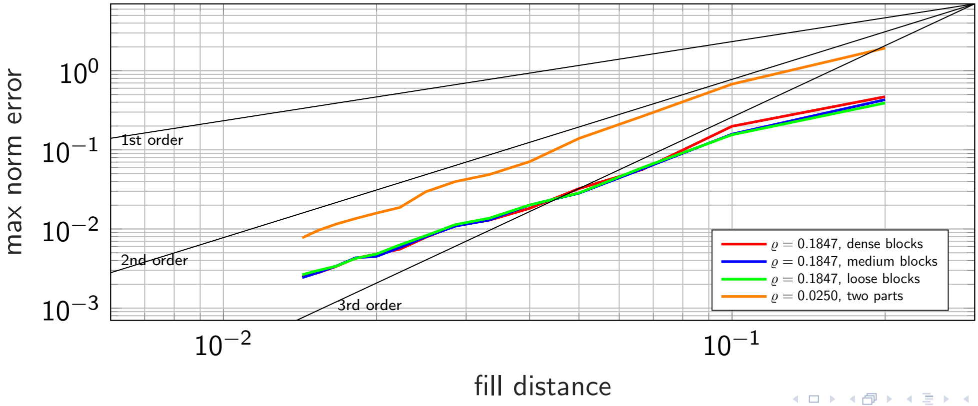

Error Graph for Discontinuous Coefficient Matrices

3d L-shaped Domain, $d = 3, p = 2, u(x_1, x_2, x_3) = (x_1 + x_2 + x_3)^4 \cos(x_1(x_1 + 2x_2 + 2x_3))$

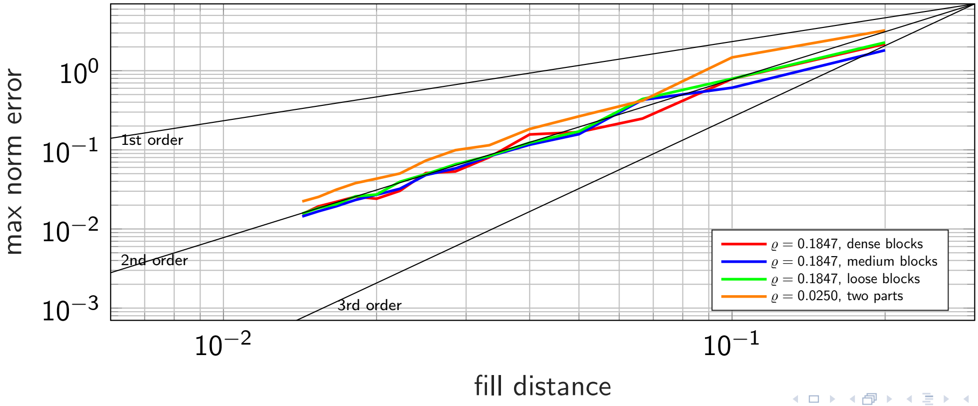

Degenerate Elliptic Equations

In the simplest case, without mutation or selection, the limiting operator of the Wright-Fisher process is the Kimura diffusion operator, with formal generator:

$$L_{\mathrm{Kim}} = \sum_{i,j=1}^{d} x_i(\delta_{ij} - x_j)\partial_{x_i}\partial_{x_j}.$$

This operator is elliptic in the interior of

$$S_d = \left\{ (x_1, x_2, \ldots, x_d) \in \mathbb{R}^d \middle| x_j \geq 0 \quad \forall j \text{ and } \sum_{j=1}^{d} x_j \leq 1 \right\}$$

but the coefficient of the second orders normal derivative tends to zero as one approaches a boundary.

Degenerate Elliptic Equations

The corresponding coefficient matrix is

$$A(\boldsymbol{x}) = \begin{pmatrix} x_1(1-x_1) & -x_1x_2 & \cdots & -x_1x_d \\ -x_2x_1 & x_2(1-x_2) & \cdots & -x_2x_d \\ \vdots & \vdots & \ddots & \vdots \\ -x_dx_1 & -x_dx_2 & \cdots & x_d(1-x_d) \end{pmatrix}.$$

It can be shown that

$$\det(A(\boldsymbol{x})) = \prod_{i=0}^{d} x_i,$$

where $x_0 = 1 - \sum_{j=1}^{d} x_j$. Thus $\det(A(\boldsymbol{x})) = 0 \iff \boldsymbol{x} \in \partial S_d$.

Degenerate Elliptic Equations

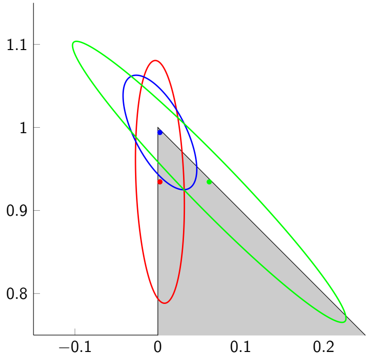

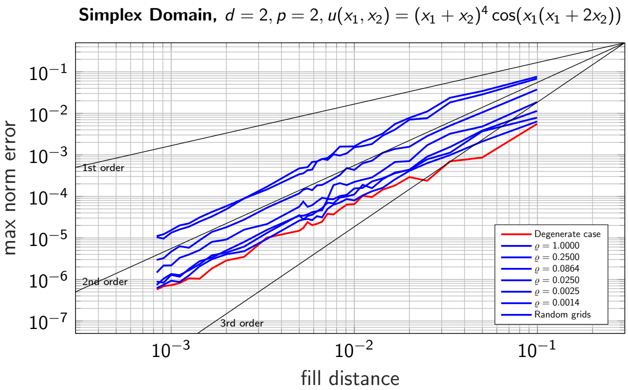

Outline

Main results

1. We have developed a meshfree method for solving non-divergence elliptic PDEs via nonlocal relaxation.
2. Minimal positive stencils are created to guarantee the numerical stability and efficiency of the method.
3. Theoretical convergence is established and second order (super)convergence is observed for $p = 2$ in practice.
4. The method can work for discontinuous coefficient matrices, non-convex domains, and near degenerate elliptic equations.
5. Our study improves the known theoretical results on the existence of positive stencils for linear elliptic equations when the ellipticity constant becomes small.

Future Work

1. Theoretical analysis for the super-convergence phenomenon.
2. High order methods; adaptive refinements; other boundary conditions.
3. Convergence analysis for degenerate elliptic equations.
4. Extensions to elliptic PDEs on manifolds and nonlinear elliptic PDEs.

Thank you

Scan to see interactive examples and more numerical results

Or visit `https://yee172.com/MPS4PDEs`

Manuscript:

`http://doi.org/10.1007/s10915-023-02294-3`

Thank you for listening!

Questions?

Research supported in part by NSF DMS-2111608 and NSF DMS-2240180

References

[Cabré, 2008] Cabré, X. (2008).
Elliptic pde's in probability and geometry: symmetry and regularity of solutions.
Discrete and Continuous Dynamical Systems, 20(3):425.

[Caffarelli and Gutiérrez, 1997] Caffarelli, L. A. and Gutiérrez, C. E. (1997).
Properties of the solutions of the linearized Monge-Ampere equation.
American Journal of Mathematics, 119(2):423–465.

[Davydov and Schaback, 2018] Davydov, O. and Schaback, R. (2018).
Minimal numerical differentiation formulas.
Numerische Mathematik, 140(3):555–592.

[Du et al., 2012] Du, Q., Gunzburger, M., Lehoucq, R. B., and Zhou, K. (2012).
Analysis and approximation of nonlocal diffusion problems with volume constraints.
SIAM review, 54(4):667–696.

[Fleming and Soner, 2006] Fleming, W. H. and Soner, H. M. (2006).
Controlled Markov processes and viscosity solutions, volume 25.
Springer Science & Business Media, New York.

[Kocan, 1995] Kocan, M. (1995).
Approximation of viscosity solutions of elliptic partial differential equations on minimal grids.
Numerische Mathematik, 72(1):73–92.

[Liu et al., 1996] Liu, W. K., Chen, Y., Jun, S., Chen, J., Belytschko, T., Pan, C., Uras, R., and Chang, C. (1996).
Overview and applications of the reproducing kernel particle methods.
Archives of Computational Methods in Engineering, 3(1):3–80.

References (cont.)

[Mirebeau, 2016] Mirebeau, J.-M. (2016).
Minimal stencils for discretizations of anisotropic pdes preserving causality or the maximum principle.
SIAM Journal on Numerical Analysis, 54(3):1582–1611.

[Mirzaei et al., 2012] Mirzaei, D., Schaback, R., and Dehghan, M. (2012).
On generalized moving least squares and diffuse derivatives.
IMA Journal of Numerical Analysis, 32(3):983–1000.

[Nochetto and Zhang, 2018] Nochetto, R. H. and Zhang, W. (2018).
Discrete abp estimate and convergence rates for linear elliptic equations in non-divergence form.
Foundations of Computational Mathematics, 18(3):537–593.

[Seibold, 2008] Seibold, B. (2008).
Minimal positive stencils in meshfree finite difference methods for the poisson equation.
Computer Methods in Applied Mechanics and Engineering, 198(3-4):592–601.

[Silling, 2000] Silling, S. A. (2000).
Reformulation of elasticity theory for discontinuities and long-range forces.
Journal of the Mechanics and Physics of Solids, 48(1):175–209.

[Trask et al., 2019] Trask, N., You, H., Yu, Y., and Parks, M. L. (2019).
An asymptotically compatible meshfree quadrature rule for nonlocal problems with applications to peridynamics.
Computer Methods in Applied Mechanics and Engineering, 343:151–165.

Proper Point Cloud

Fill Distance:

$$h = \inf \left\{ h : \overline{\Omega_\delta} \subseteq \bigcup_{i=1}^{M} \overline{B_h(\boldsymbol{x}_i)} \right\}$$
$$= \sup_{\boldsymbol{x} \in \overline{\Omega_\delta}} \min_{1 \le i \le M} |\boldsymbol{x} - \boldsymbol{x}_i|.$$

Use **Voronoi diagram**.

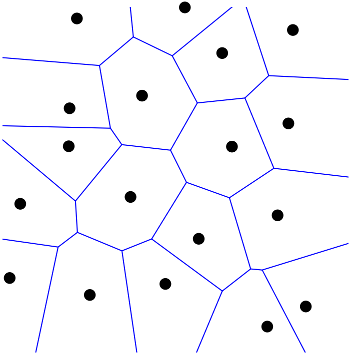

Proper Point Cloud (cont.)

When we say a point cloud is proper, we mean

1. Fill distance is small enough;
2. Separation between interior points is large enough;
3. Proportional to the fill distance, there are no interior points too close to the boundary.

In short, we want the points in the point cloud to be as evenly distributed as possible (each point is not too far away from or too close to its neighbors).

Cone Condition

Theorem 3 (Seibold, 2008)

Take a point cloud $X = \{\boldsymbol{x}_i\}_{i=1}^M \subset \Omega_\delta \subset \mathbb{R}^d$ and let $\boldsymbol{x}_i \in \Omega$ be fixed. If for any unit vector $\boldsymbol{v} \in \mathbb{R}^d$, $\mathcal{C}_\delta^{\boldsymbol{v}}(\boldsymbol{x}_i) \cap X \setminus \{\boldsymbol{x}_i\} \neq \emptyset$, then the feasible set with $A(\boldsymbol{x}) = I_{d\times d}$ and $p = 2$ is not empty.

The cone $\mathcal{C}_\delta^{\boldsymbol{v}}(\boldsymbol{x}_i)$ in $B_\delta(\boldsymbol{x}_i)$ is defined as

$$\mathcal{C}_\delta^{\boldsymbol{v}}(\boldsymbol{x}_i) := \left\{ \boldsymbol{x} \in B_\delta(\boldsymbol{x}_i) : \boldsymbol{x}^T \boldsymbol{v} \geq \frac{1}{\sqrt{1+\sigma_d}} |\boldsymbol{x}|^2 \right\}$$

where $\sigma_d = \sqrt{2} - 1$ (a cone with total opening angle 45°) for $d = 2$ and $\sigma_d = \sqrt{(3-\sqrt{6})/6}$ (a cone with total opening angle 33.7°) for $d = 3$.

Cone Condition (cont.)

Using mapping, we can extend the cone condition to the general case.

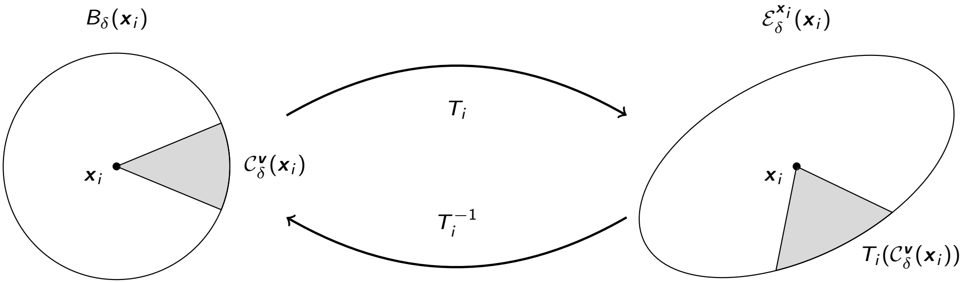

Cone Condition (cont.)

By the definition of the fill distance, there are no holes with a radius larger than h. We can estimate how large the searching area is needed. We can prove that $r(\varrho) = \Theta(\sqrt{\varrho})$.